Suppression of fluorescence phonon sideband from nitrogen vacancy centers in diamond nanocrystals by substrate effect

Hong-Quan Zhao,[1,2] Masazumi Fujiwara,[1,2] and Shigeki Takeuchi[1,2,*]

[1]*Research Institute for Electronic Science, Hokkaido University, Sapporo 060-0812, Japan*
[2]*The Institute of Scientific and Industrial Research, Osaka University, Osaka 567-0047, Japan*
[*]*takeuchi@es.hokudai.ac.jp*

Abstract: Substrates effect is observed on the suppression of the phonon sideband from nitrogen vacancy (NV) centers in 50nm diamond nanocrystals at cryogenic temperatures. As a quantitative parameter of the population of phonon sidebands, the Debye–Waller factor is estimated from fluorescence spectra on glass, silicon, and silica-on-silicon substrates. Fluorescence spectra of negatively charged NV centers in nanodiamonds on silica-on-silicon substrates have average and maximum Debye–Waller factors of 12.7% (which is about six times greater than that of samples on glass substrates) and 19.3%, respectively. This effect is expected to be very important for future applications of NV centers in quantum information science and nanosensing.

OCIS codes: (300.0300) Spectroscopy; (300.2530) Fluorescence, laser-induced; (160.2220) Defect-center materials.

References and links

1. F. Jelezko and J. Wrachtrup, "Single defect centres in diamond: A review," Phys. Status Solidi **203**(13), 3207–3225 (2006) (a).
2. Y. S. Park, A. K. Cook, and H. L. Wang, "Cavity QED with diamond nanocrystals and silica microspheres," Nano Lett. **6**(9), 2075–2079 (2006).
3. L. Childress, M. V. Gurudev Dutt, J. M. Taylor, A. S. Zibrov, F. Jelezko, J. Wrachtrup, P. R. Hemmer, and M. D. Lukin, "Coherent dynamics of coupled electron and nuclear spin qubits in diamond," Science **314**(5797), 281–285 (2006).
4. A. Batalov, V. Jacques, F. Kaiser, P. Siyushev, P. Neumann, L. J. Rogers, R. L. McMurtrie, N. B. Manson, F. Jelezko, and J. Wrachtrup, "Low temperature studies of the excited-state structure of negatively charged nitrogen-vacancy color centers in diamond," Phys. Rev. Lett. **102**(19), 195506 (2009).
5. Ph. Tamarat, T. Gaebel, J. R. Rabeau, M. Khan, A. D. Greentree, H. Wilson, L. C. L. Hollenberg, S. Prawer, P. Hemmer, F. Jelezko, and J. Wrachtrup, "Stark shift control of single optical centers in diamond," Phys. Rev. Lett. **97**(8), 083002 (2006).
6. Y. M. Shen, T. M. Sweeney, and H. L. Wang, "Zero-phonon linewidth of single nitrogen vacancy centers in diamond nanocrystals," Phys. Rev. B **77**(3), 033201 (2008).
7. P. Siyushev, V. Jacques, I. Aharonovich, F. Kaiser, T. Müller, L. Lombez, M. Atatüre, S. Castelletto, S. Prawer, F. Jelezko, and J. Wrachtrup, "Low-temperature optical characterization of a near-infrared single-photon emitter in nanodiamonds," New J. Phys. **11**(11), 113029 (2009).
8. M. Barth, S. Schietinger, T. Schröder, T. Aichele, and O. Benson, "Controlled coupling of NV defect centers to plasmonic and photonic nanostructures," J. Lumin. **10**, 1016 (2010).
9. T. D. Ladd, F. Jelezko, R. Laflamme, Y. Nakamura, C. Monroe, and J. L. O'Brien, "Quantum computers," Nature **464**(7285), 45–53 (2010).
10. K. Kojima, H. F. Hofmann, S. Takeuchi, and K. Sasaki, "Nonlinear interaction of two photons with a one-dimensional atom: spatiotemporal quantum coherence in the emitted field," Phys. Rev. A **68**(1), 013803 (2003).
11. H. F. Hofmann, K. Kojima, S. Takeuchi, and K. Sasaki, "Entanglement and four-wave mixing effects in the dissipation-free nonlinear interaction of two photons at a single atom," Phys. Rev. A **68**(4), 043813 (2003).
12. M. Fujiwara, K. Toubaru, T. Noda, H.-Q. Zhao, and S. Takeuchi, "Highly efficient coupling of photons from nanoemitters into single-mode optical fibers," Nano Lett. **11**(10), 4362–4365 (2011).
13. C.-H. Su, A. D. Greentree, and L. C. L. Hollenberg, "Towards a picosecond transform-limited nitrogen-vacancy based single photon source," Opt. Express **16**(9), 6240–6250 (2008).
14. E. Knill, R. Laflamme, and G. J. Milburn, "A scheme for efficient quantum computation with linear optics," Nature **409**(6816), 46–52 (2001).

#165559 - $15.00 USD Received 29 Mar 2012; revised 24 May 2012; accepted 5 Jun 2012; published 26 Jun 2012

15. T. Nagata, R. Okamoto, J. L. O'brien, K. Sasaki, and S. Takeuchi, "Beating the standard quantum limit with four-entangled photons," Science **316**(5825), 726–729 (2007).
16. R. Okamoto, J. L. O'Brien, H. F. Hofmann, T. Nagata, K. Sasaki, and S. Takeuchi, "An entanglement filter," Science **323**(5913), 483–485 (2009).
17. R. Okamoto, J. L. O'Brien, H. F. Hofmann, and S. Takeuchi, "Realization of a Knill-Laflamme-Milburn controlled-NOT photonic quantum circuit combining effective optical nonlinearities," Proc. Natl. Acad. Sci. U.S.A. **108**(25), 10067–10071 (2011).
18. T. M. Babinec, B. J. M. Hausmann, M. Khan, Y. N. Zhang, J. R. Maze, P. R. Hemmer, and M. Loncar, "A diamond nanowire single-photon source," Nat. Nanotechnol. **5**(3), 195–199 (2010).
19. L. Childress, M. V. Gurudev Dutt, J. M. Taylor, A. S. Zibrov, F. Jelezko, J. Wrachtrup, P. R. Hemmer, and M. D. Lukin, "Coherent Dynamics of Coupled Electron and Nuclear Spin Qubits in Diamond," Science **314**(5797), 281–285 (2006).
20. T. Schröder, F. Gädeke, M. J. Banholzer, and O. Benson, "Ultrabright and efficient single-photon generation based on nitrogen-vacancy centres in nanodiamonds on a solid immersion lens," New J. Phys. **13**(5), 055017 (2011).
21. J. Wolters, A. W. Schell, G. Kewes, N. Nüsse, M. Schoengen, H. Döscher, T. Hannappel, B. Löchel, M. Barth, and O. Benson, "Enhancement of the zero phonon line emission from a single nitrogen vacancy center in a nanodiamond via coupling to a photonic crystal cavity," Appl. Phys. Lett. **97**(14), 141108 (2010).
22. S. Schietinger, M. Barth, T. Aichele, and O. Benson, "Plasmon-enhanced single photon emission from a nanoassembled metal-diamond hybrid structure at room temperature," Nano Lett. **9**(4), 1694–1698 (2009).
23. A. Faraon, P. E. Barclay, C. Santori, K.-M. C. Fu, and R. G. Beausoleil, "Resonant enhancement of the zero-phonon emission from a colour centre in a diamond cavity," Nat. Photonics **5**(5), 301–305 (2011).
24. Y. S. Park, A. K. Cook, and H. L. Wang, "Cavity QED with diamond nanocrystals and silica microspheres," Nano Lett. **6**(9), 2075–2079 (2006).
25. R. H. Silsbee, "Thermal broadening of the Mössbauer line and of narrow-line electronic spectra in solids," Phys. Rev. **128**(4), 1726–1733 (1962).
26. M. N. Sapozhnikov, "Zero-phonon transitions in the optical spectra of impurity molecular crystals," Phys. Status Solidi **75**(1), 11–51 (1976) (b).
27. J. R. Maze, P. L. Stanwix, J. S. Hodges, S. Hong, J. M. Taylor, P. Cappellaro, L. Jiang, M. V. G. Dutt, E. Togan, A. S. Zibrov, A. Yacoby, R. L. Walsworth, and M. D. Lukin, "Nanoscale magnetic sensing with an individual electronic spin in diamond," Nature **455**(7213), 644–647 (2008).
28. D. Englund, B. Shields, K. Rivoire, F. Hatami, J. Vučković, H. Park, and M. D. Lukin, "Deterministic coupling of a single nitrogen vacancy center to a photonic crystal cavity," Nano Lett. **10**(10), 3922–3926 (2010).
29. J. R. Rabeau, A. Stacey, A. Rabeau, S. Prawer, F. Jelezko, I. Mirza, and J. Wrachtrup, "Single nitrogen vacancy centers in chemical vapor deposited diamond nanocrystals," Nano Lett. **7**(11), 3433–3437 (2007).
30. C. Kurtsiefer, B. Mayer, S. Zarda, and H. Weinfurter, "Stable solid-state source of single photons," Phys. Rev. Lett. **85**(2), 290–293 (2000).
31. H-Q, Zhao, M. Fujiwara, and S. Takeuchi, Research Institute of Electronic Science, Hokkaido University, 8–1 Mihogaoka, Ibaraki, Osaka, JAPAN, 567–0047, are preparing a manuscript to be called "Temperature dependence of fluorescence spectra of nitrogen vacancy centers in diamond nanocrystals deposited on different substrates."

1. Introduction

Nitrogen vacancy (NV) centers have excited great interest in recent years as they have many advantageous properties including robustness, optical transitions with long coherence times, and very long spin coherence times [1–5]. Of the many advantageous optical properties of NV centers, zero-phonon transitions in fluorescence spectra have been extensively investigated both theoretically and experimentally [6–8]. These transitions give rise to a very narrow zero-phonon line (ZPL) with a line width of tens of MHz [6]. The ZPL of negatively charged NV centers in nanodiamonds have been known to be particularly prospective in the future quantum information processing [9], photonic quantum memories/gates [10], and nano magnetic sensors [11]. For example, it allows the generation of a narrow-band indistinguishable single photons [12] needed for quantum computation [13,14], quantum repeaters and quantum metrology [15–17].

Unlike NV centers in bulk diamond crystals, NV centers in nanodiamonds can be used to fabricate nanodevices using a bottom-up approach [18–20]. However, NV centers in nanodiamonds suffer from strong phonon sidebands, even at cryogenic temperatures [21]. These broad and intense phonon sidebands are very detrimental in quantum optical systems since the high probability of a transition to the phonon sidebands greatly reduces the probability of the zero-phonon transition in a two-level system. Techniques for overcoming this problem include enhancing the zero-phonon transition by coupling to the modes of

#165559 - $15.00 USD Received 29 Mar 2012; revised 24 May 2012; accepted 5 Jun 2012; published 26 Jun 2012

optical microcavities or waveguides using the Purcell effect [22–24], and succeeded in enhancing the fraction of NV emission into ZPL from about 3% to 16%.

As a simple alternative method, here, we report that certain substrates suppress phonon sidebands of NV centers in diamond nanocrystals. We found that the phonon sidebands are strongly suppressed when diamond nanocrystals are distributed on silicon or silica-on-silicon substrates. As a quantitative parameter of the phonon sideband population, the Debye–Waller factors [25,26] of diamond nanocrystals on glass, silicon, and silica-on-silicon substrates are estimated from their fluorescence spectra. Samples on silica-on-silicon substrates are estimated to have an average Debye–Waller factor of 12.7%, which is six times greater than that of samples on glass substrates. A maximum Debye-Waller factor of 19.3% is recorded. This is expected to be very important for applications of NV centers in quantum information science and nanosensing [27].

2. Experimental methods and setups

Type Ib diamond nanocrystals (Microdiamant GMBH) with an average size of 50 nm were used in the present experiments. NV centers naturally existed in some diamond nanocrystals. Monocrystalline suspensions of these diamonds were purified by centrifuging 10 times. The nanodiamonds were deposited on glass (thickness: 170 μm), undoped Si (thickness: 250 μm), and SiO_2 (~2 μm) on Si (250 μm) (SiO_2/Si) substrates. These substrates were organically cleaned by a dilute aqueous detergent (SCAT 20X-N) to remove any organic contamination and they were then repeatedly rinsed in deionized water by ultrasonic cleaning to remove any residual water-soluble organic solvent. The substrate surfaces were then made hydrophilic to realize a uniform distribution of diamond nanocrystals (for glass slides: $HCl:H_2O$ = 1:5; room temperature; 10 min; for Si: $NaOH:H_2O$ = 1:5; room temperature; 10 min). Diamond nanocrystals were then spin coated on the substrate surfaces. The substrates were attached to the cold finger of a cryostat (Microstat, Oxford Instruments).

A home-made laser scanning confocal microscope (Fig. 1) was used to obtain images. The microscope used a continuous-wave green (543.5 nm) laser for pumping. The polarization of the incident pump beam was converted from linear to circular by a quarter-wave plate. The beam was then collimated and focused by an objective lens (LCPLFLN-LCD, Olympus; numerical aperture: 0.7). We employed a pinhole whose diameter of 20 μm was very close to the width of the laser beam waist at the focal point to increase the signal-to-noise ratio. Diamond crystals containing NV centers were then irradiated by a focused laser spot with a diameter of about 800 nm. The cryostat was stiffly mounted on a heavy optical table to prevent the cryostat from vibrations coming from liquid helium transfer tube. The laser focus spots did not drift noticeably over a typical data accumulation time of about 10 min. The confocal system is controlled by a mechanical motor controller with three degrees of freedom and a precision of 100 nm. When necessary, a Hanbury-Brown and Twiss (HBT) [6] interferometer was used to further confirm the presence of single or multiple NV centers by checking second-order photon correlation histograms ($g^{(2)}(\tau)$). The SEM image shows two diamond nanocrystals (red arrow pointed) uniformly deposited on the substrate. Figure 2(a) shows a laser scanning image of a single 50 nm diamond crystal on a SiO_2/Si substrate obtained at 4 K with a step size of 300 nm. In this image, the red circle indicates the signal from NV centers; the number of NV centers in the spot can be estimated from the $g^{(2)}(0)$ dip of the fluorescence photon antibunching function (Fig. 2(b)) [28,29]. The red curve in Fig. 2(b) shows the theoretical fit to the data obtained by assuming a three-level system in nanodiamonds [30]. Figure 2(c) shows fluorescence spectra of NV centers in the spot. Some ZPL peaks may be indistinguishable in Fig. 2(c) due to the limited resolution of the spectrometer.

#165559 - $15.00 USD Received 29 Mar 2012; revised 24 May 2012; accepted 5 Jun 2012; published 26 Jun 2012

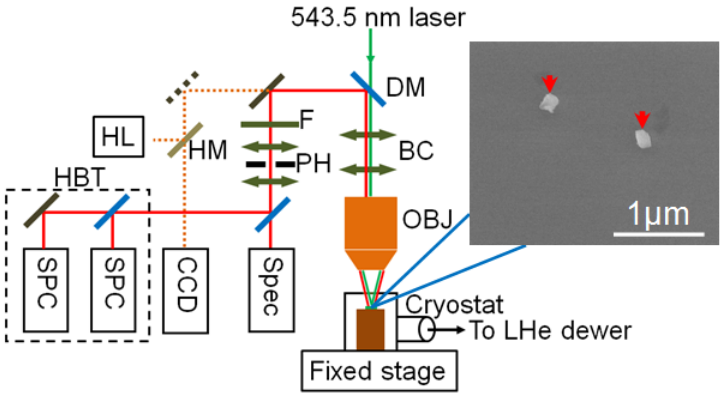

Fig. 1. Stable home-made confocal microscope system with a cryostat installed on a fixed stage. The inserted SEM image shows a uniform distribution of average ~50 nm of diamonds on the substrate, the red-arrows indicating the nanodiamonds. (DM: dichroic mirror; BC: beam control; OBJ: objective lens; F: filter; PH: pinhole; HM: half mirror; HL: halogen-tungsten lamp; Spec: spectrometer; HBT: Hanbury-Brown and Twiss_interferometer; CCD: Charge Coupled Device; SPC: Single Photon Counter).

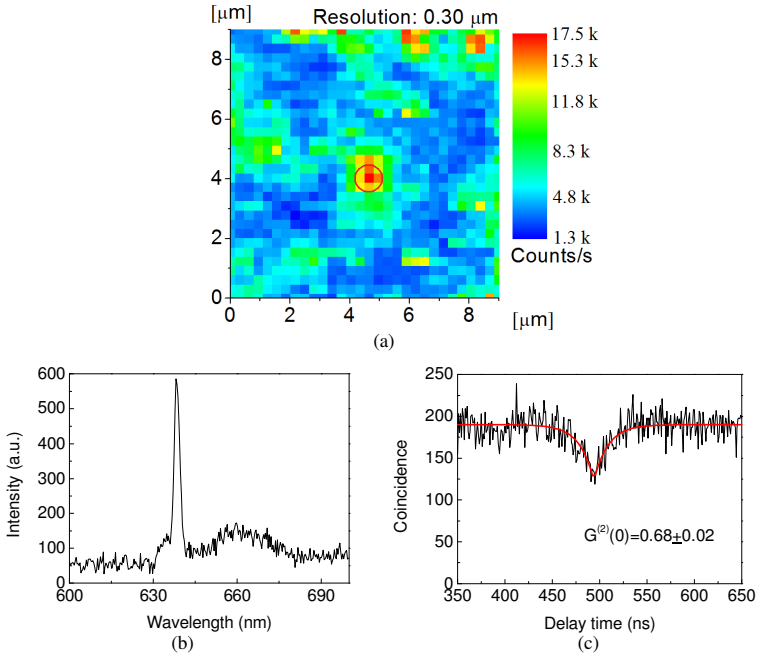

Fig. 2. (a) Laser confocal microscopy image of 50-nm diamond crystals. (b) NV center fluorescence photon antibunching function (measured from the nanodiamond indicated by the red circle in (a)). The red curve is a theoretical fit to the data for a three-level system. (c) Spectrum obtained from this multiple NV center in the same nanodiamond.

3. Results and discussion

We first measured the fluorescence spectra of NV centers on the three different substrates at room temperature (RT) (Figs. 3(a)–3(c)). The excitation intensity was 2×10^5 W/cm^2. Figure 3(a) shows the fluorescence spectrum obtained from the sample on the glass slide. The NV^- centers gave a ZPL with a very weak intensity and also a broad and intense phonon sideband

#165559 - $15.00 USD Received 29 Mar 2012; revised 24 May 2012; accepted 5 Jun 2012; published 26 Jun 2012

spectrum. Figure 3(b) shows a similar NV spectrum from a sample on a Si substrate. The ZPL is a little stronger than that of the sample on the glass substrate. Figure 3(c) shows the spectrum of NV centers in sample on the silica-on-silicon substrate. This spectrum has a similar profile to that of the sample on the glass substrate. The Debye–Waller factors measured from the ZPL in all these obtained fluorescence spectra were less than 1%, as discussed below.

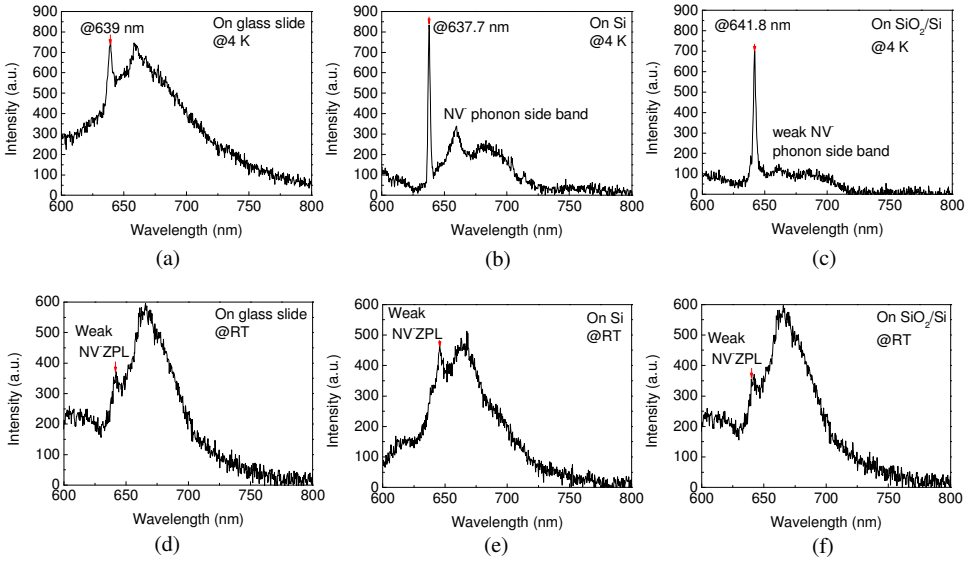

Fig. 3. Spectra of NV centers in diamond nanocrystals measured at (a)–(c) RT and (d)–(f) 4 K on (a) and (d) glass, (b) and (e) Si, and (c) and (f) SiO_2/Si substrates.

Figures 3(d)–3(f) show spectra of NV centers measured at 4 K. Figure 3(d) shows the spectrum from NV centers in the sample on a glass substrate. The Debye–Waller factor of ZPL is slightly enhanced relative to that of the RT spectrum. Note that the ZPL width is determined by the spectrometer resolution (2 nm). In contrast, a very sharp ZPL was obtained for the sample on Si substrates, as shown in Fig. 3(e). The phonon sideband is greatly suppressed compared to that for the glass substrate. Interestingly, the phonon sideband of the sample on the SiO_2/Si substrate (Fig. 3(f)) was further suppressed; the phonon sideband intensity was half that of the sample on the Si substrate with a similar ZPL intensity.

For more quantitative analysis, in this study, the Debye–Waller factor $F_{D\text{-}W}$ was calculated using the following function:

$$F_{D-W} = \frac{\int d\lambda I_{ZPL}}{\int d\lambda I_{ZPL} + \int d\lambda I_{Phonon-sideband}} \quad (1)$$

This is schematically depicted in Fig. 4. The NV^- ZPL Debye–Waller factor is calculated to be ~1% for the sample on the glass substrate, even at 4 K. In contrast, the sample on the Si substrate has a Debye–Waller factor of 8.47%, which is eight times greater than that of the sample on the glass sample. Furthermore, the sample on the SiO_2/Si substrate has a Debye–Waller factor of 19.3%, which is more than twice that of the sample on the Si substrate.

#165559 - $15.00 USD Received 29 Mar 2012; revised 24 May 2012; accepted 5 Jun 2012; published 26 Jun 2012

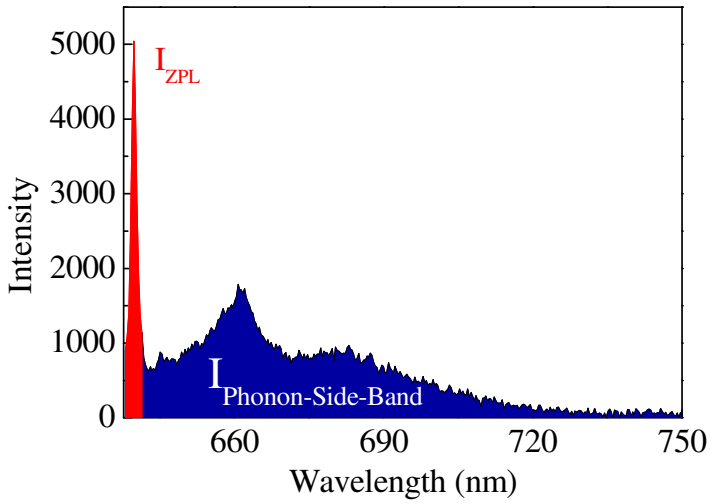

Fig. 4. Method for calculating the Debye–Waller factor from NV center fluorescence spectra.

To investigate this suppression of the phonon sideband in more detail, we repeated the measurements of the NV center fluorescence spectra and obtained statistical distributions of $F_{D\text{-}W}$ for the three substrates (Fig. 5). Here, 16 samples were selected on each substrate (total 48 samples) with a single ZPL in the fluorescence spectrum. The NV^- ZPL of the samples on glass substrates gave Debye–Waller factors in the range 1 to 3%. The average Debye–Waller factor for all 16 samples is 2%. For samples on undoped Si substrates, the Debye–Waller factors obtained from the NV^- ZPL are distributed over a wider range of 3 to 13%. The distribution peaks between 5 and 7% and the average Debye–Waller factor is 7.3%. Samples on SiO_2/Si substrates exhibit a similar wide distribution with Debye–Waller factors in the range 9 to 19%. The distribution peaks between 11 and 13% and the average Debye–Waller factor is 12.7%. The largest Debye–Waller factor observed in this experiment was 19.3%. The average Debye–Waller factor of samples on SiO_2/Si substrates is almost six times greater than those of samples on glass substrates and is twice those of samples on Si substrates. These experimental results clearly demonstrate that some substrates can suppress the phonon sideband of NV centers in diamond nanocrystals.

We considered whether local heating of the samples by the pump laser beam may have caused the above-mentioned differences since the substrates had different thermal conductivities. To determine whether this was the case, we measured the Debye–Waller factors from the NV^- ZPL of the three substrates at 4 K using five different excitation intensities (2×10^5, 1×10^5, 0.5×10^5, 0.2×10^5, and 0.1×10^5 W/cm^2). Figure 6 shows the results obtained. Even when the excitation intensity was varied by a factor of 20, the variation in the Debye–Waller factors was lower for the same substrate than that between different substrates. We thus conclude that local heating by the pump laser is not the main cause of the observed differences in the Debye–Waller factors for the different substrates. After the submission of this paper, we found that the Debye-Waller factors for the samples on Si and SiO2/Si decreased linearly as the temperature increased from 4 K to 230 K (The details will be reported elsewhere [31].)

It may be possible that the strain inside the nano crystal may be related to the observed differences in the Debye-Waller factors for the different substrates. In order to study this possibility, further investigation on polarization anisotropy will be helpful. It will be also interesting to study the relation between the Debye-Waller factors and the size of the nano diamonds in future.

#165559 - $15.00 USD Received 29 Mar 2012; revised 24 May 2012; accepted 5 Jun 2012; published 26 Jun 2012

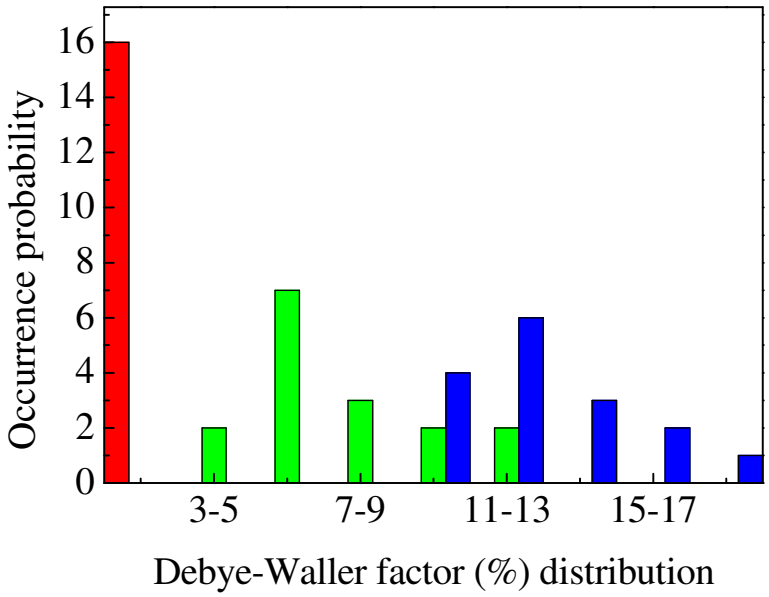

Fig. 5. Statistical distribution of NV^- ZPL Debye–Waller factors for samples based on the three different substrates. The red, green, and blue bars represent the $F_{D\text{-}W}$ distributions of samples on glass, undoped Si, and SiO_2/Si substrates, respectively.

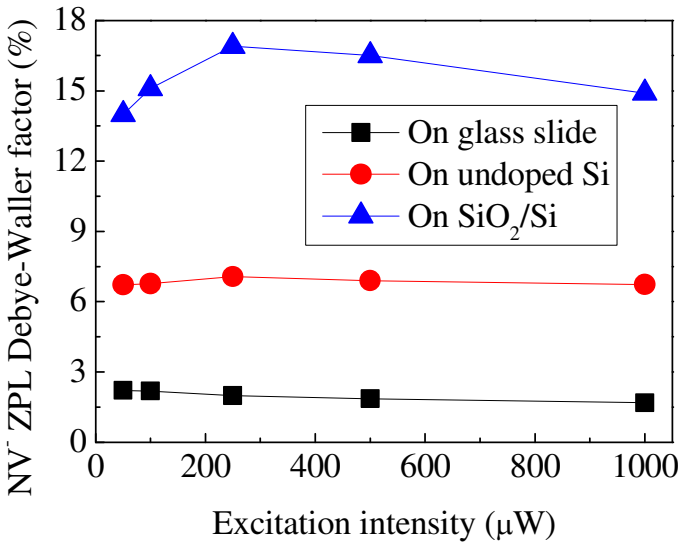

Fig. 6. NV^- Debye–Waller factors as a function of excitation power for samples on glass (black), undoped Si (red), and SiO_2/Si (blue) substrates.

4. Conclusion

Substrates effect is observed on the suppression of the phonon sideband from nitrogen vacancy (NV) centers in 50nm diamond nanocrystals at cryogenic temperatures. As a quantitative parameter of the population of phonon sidebands, the Debye–Waller factor is estimated from fluorescence spectra on glass, silicon, and silica-on-silicon substrates. Fluorescence spectra of negatively charged NV centers in nanodiamonds on silica-on-silicon

#165559 - $15.00 USD Received 29 Mar 2012; revised 24 May 2012; accepted 5 Jun 2012; published 26 Jun 2012

substrates have average and maximum Debye–Waller factors of 12.7% (which is about six times greater than that of samples on glass substrates) and 19.3%, respectively. This effect is expected to be very important for future applications of NV centers in quantum information science and nanosensing.

Acknowledgments

We thank Prof. M. Takahashi for his helpful comments on the sample spin-coating method. We gratefully acknowledge financial support from MEXT-KAKENHI Quantum Cybernetics (No. 21101007), JSPS-KAKENHI (Nos. 20244062, 21840003, 23244079, and 23740228), JST-CREST, JSPS-FIRST, MIC-SCOPE, Project for Developing Innovation Systems of MEXT, G-COE Program, and the Research Foundation for Opto-Science and Technology.

#165559 - $15.00 USD Received 29 Mar 2012; revised 24 May 2012; accepted 5 Jun 2012; published 26 Jun 2012